A neutron and x-ray diffraction study of calcium aluminate glasses

2003 J. Phys.: Condens. Matter 15 S2413

(http://iopscience.iop.org/0953-8984/15/31/316)

INSTITUTE OF PHYSICS PUBLISHING JOURNAL OF PHYSICS: CONDENSED MATTER

J. Phys.: Condens. Matter **15** (2003) S2413–S2423 PII: S0953-8984(03)63549-6

A neutron and x-ray diffraction study of calcium aluminate glasses

C J Benmore[1,4], J K R Weber[2], S Sampath[1,3], J Siewenie[1], J Urquidi[1] and J A Tangeman[2]

[1] Intense Pulsed Neutron Source, Argonne National Laboratory, IL 60439, USA
[2] Containerless Research Incorporated, 906 University Place, Evanston, IL 60201, USA
[3] Department of Chemistry, University of Wyoming, Laramie, WY 82071, USA

E-mail: Benmore@anl.gov

Received 16 May 2003
Published 23 July 2003
Online at stacks.iop.org/JPhysCM/15/S2413

Abstract

Spallation neutron diffraction and high-energy x-ray diffraction methods have been used to study $CaO:Al_2O_3$ glasses at the 64:36 mol% eutectic and 50:50 mol% compositions. The samples were produced by the containerless cooling of liquid droplets heated by a laser beam and suspended in an aerodynamic levitator. The results show aluminium on average to be surrounded by 4.0(1) oxygen atoms at a distance of 1.76(1) Å in $CaAl_2O_4$, which increases to 4.8(1) at the eutectic composition. The two techniques have also been combined to reveal the local structure of the calcium atoms in the glass. In $CaAl_2O_4$ the calcium is found to be surrounded, on average, by 5.6(2) oxygen atoms at a distance of 2.38 Å. The Ca coordination decreases to the unusually low value of 3.9(2) oxygen atoms at a distance of 2.40 Å at the eutectic composition. No additional Ca–O correlations are observed up to 2.7 Å, but longer bonds cannot be ruled out. The higher-r correlations are shown to be similar in the two glasses, suggesting that both Al and Ca may act as network formers. The results are compared to previous studies on splat-quenched glasses with compositions near the eutectic.

1. Introduction

Liquids formed from binary $CaO–Al_2O_3$ (CA) materials [1, 2] can be vitrified to form hard, transparent, colourless glasses [3, 4]. The glasses exhibit infrared transmission to about 5500 nm and are potentially useful as a laser host and infrared optical material [5–7]. Many crystalline calcium aluminate phases are of interest from the geological standpoint and are common components of hydraulic cements [8].

[4] Author to whom any correspondence should be addressed.

Hannon and Parker [4] studied the structure of splat-quenched calcium aluminate glasses containing 30 and 38 mol% Al_2O_3 by means of high-resolution pulsed neutron diffraction. The structure factors showed similar features in the two materials. An Al–O bond length of ∼1.76 Å and coordination number of 4.0 were measured, and no significant distortion of the AlO_4^{5-} tetrahedra was detected. The Ca–O peak at 2.34 Å was also found to give a coordination number of 4.0, which is smaller than expected from bond valence theory calculations. These results suggested that higher-coordinate species were also present, but this could not be confirmed due to overlap between the Ca–O and O–O correlations [4]. Morikawa *et al* [9] performed conventional x-ray diffraction measurements on a 36.8 mol% Al_2O_3 splat-quenched glass and calculated the Al and Ca coordination numbers to be 4.2 and 5.6 at distances of 1.77 and 2.37 Å, respectively. The apparent disparities between the prior measurements suggest that the Ca, and possibly the Al, ions can accommodate a range of structures in the glass, which are sensitive to the glass synthesis conditions.

Poe *et al* [3, 10] performed ion dynamics simulations and *in situ* ^{27}Al NMR spectroscopy to study the aluminium ion environment in glass and liquid CA binaries containing 30–70 mol% Al_2O_3. The simulation results indicated that the average coordination of Al in the liquids increases from ∼4 to 5 with increasing Al content, with $n_{\mathrm{Al}}^{\mathrm{O}} = 4.2$ at the eutectic composition and $n_{\mathrm{Al}}^{\mathrm{O}} = 4.5$ at the equimolar composition (where $n_{\mathrm{Al}}^{\mathrm{O}}$ represents the coordination of Al by O). NMR measurements on the glasses indicated that a mixture of Al ion environments also occurred in the glass [3].

In this study an aerodynamic levitation system combined with laser heating has been used to fabricate the glassy samples. The materials investigated in this work were 64:36 and 50:50 mol% $CaO:Al_2O_3$. The former composition corresponds to a pseudo-binary eutectic between $Ca_3Al_2O_6$ (C3A) and $CaAl_2O_4$ (CA) as reported by Nurse *et al* [2]. However, we note that Christensen [11] has also reported a line phase, mayenite $Ca_{12}Al_{14}O_3$, at a composition close to the 64:36 mol% CA eutectic. Combined neutron and high-energy x-ray diffraction experiments were performed on the same samples to obtain a detailed picture of glass structure. Since neutrons are particularly sensitive to the positions of the lighter oxygen atoms and x-ray scattering is more sensitive to the positions of the heavier Ca and Al component interactions, these two techniques are highly complementary in the case of oxide glasses.

2. Theory

The quantity measured in a neutron diffraction experiment is the differential cross-section:

$$\frac{\mathrm{d}\sigma}{\mathrm{d}\Omega} = \frac{\mathrm{d}\sigma}{\mathrm{d}\Omega}_{\mathrm{self}} + \frac{\mathrm{d}\sigma}{\mathrm{d}\Omega}_{\mathrm{distinct}} = \sum_{\alpha} c_\alpha b_\alpha^2 + P(\theta) + F_{\mathrm{N}}(Q) \tag{1}$$

where $P(\theta)$ is the inelastic scattering contribution and $F_{\mathrm{N}}(Q)$ is the total scattering structure factor arising from the 'distinct scattering' contribution, c_α is the atomic concentration and b_α the scattering length of isotope α.

$$S_{\mathrm{N}}(Q) = \frac{F_{\mathrm{N}}(Q)}{\left(\sum_\alpha c_\alpha b_\alpha\right)^2} = \frac{1}{\left(\sum_\alpha c_\alpha b_\alpha\right)^2} \sum_{\alpha,\beta} c_\alpha b_\alpha c_\beta b_\beta (S_{\alpha\beta}(Q) - 1) \tag{2}$$

where $S_{\mathrm{N}}(Q)$ is the total neutron static structure factor and $S_{\alpha\beta}(Q)$ are the Faber–Ziman partial structure factors (see tables 1 and 2) [12].

Similarly, in an x-ray diffraction experiment,

$$\frac{\mathrm{d}\sigma}{\mathrm{d}\Omega} = \frac{\mathrm{d}\sigma}{\mathrm{d}\Omega}_{\mathrm{Compton}} + \frac{\mathrm{d}\sigma}{\mathrm{d}\Omega}_{\mathrm{self}} + \frac{\mathrm{d}\sigma}{\mathrm{d}\Omega}_{\mathrm{distinct}} = C_{\mathrm{X}}(Q) + \sum_{\alpha} c_\alpha f_\alpha^2(Q) + I_{\mathrm{X}}(Q) \tag{3}$$

Table 1. The normalized neutron and x-ray (at $Q = 0$ Å^{-1}) Faber–Ziman weighting factors for CA eutectic. Note that the Ca–O and Al–O weighting factors for the 64:36 composition are almost identical. Whilst the O–O is the dominant neutron contribution, the Ca and Al interactions are more significant in the x-ray spectra.

Sample/technique	Ca–Ca	Ca–Al	Ca–O	Al–Al	Al–O	O–O
64:36 neutron	0.038	0.063	0.253	0.026	0.206	0.414
64:36 x-ray	0.127	0.186	0.273	0.068	0.199	0.147
50:50 neutron	0.019	0.054	0.182	0.039	0.263	0.443
50:50 x-ray	0.066	0.171	0.211	0.111	0.272	0.169

where $C_X(Q)$ is the Compton scattering contribution which asymptotically approaches the number of electrons at high Q, $f_\alpha(Q)$ are the Q-dependent atomic form factors and $I_X(Q)$ represents the distinct scattering. The pseudo-nuclear, total x-ray static structure factor $S_X(Q)$ can be calculated within the independent atom approximation using

$$S_X(Q) = \frac{I_X(Q)}{\left(\sum_\alpha c_\alpha f_\alpha(Q)\right)^2} = \frac{1}{\left(\sum_\alpha c_\alpha f_\alpha(Q)\right)^2} \sum_{\alpha,\beta} c_\alpha f_\alpha(Q) c_\beta f_\beta(Q)(S_{\alpha\beta}(Q) - 1). \tag{4}$$

The term pseudo-nuclear is used here as it is assumed that the electron density of each atom is spherical in order to deduce the nuclear positions. The measured neutron and x-ray $S(Q)$ is related to the total radial distribution function $G(r)$ via a Fourier transform, given by

$$S(Q) = 1 + \frac{4\pi\rho}{Q} \int_0^\infty r\, \mathrm{d}r (G(r) - 1) \sin(Qr) \tag{5}$$

where ρ is the atomic number density and Q is the momentum transfer divided by $\hbar$.

In this study we have combined the x-ray and neutron data sets to extract or eliminate specific partial structure factors using the equation

$$\Delta S(Q) = \frac{[S_X(Q) - 1] - \frac{W_X(Q)}{W_N}[S_N(Q) - 1]}{1 - \left(\frac{W_X(Q)}{W_N}\right)} \tag{6}$$

where W represents the Faber–Ziman weighting factors for neutrons W_N and x-rays $W_X(Q)$. The $\Delta S(Q)$ function was constructed to eliminate the $S_{OO}(Q)$ contribution, as a means to resolve information on the CaO interactions (see table 1).

3. Experimental details

The glass samples were made by the containerless melting and cooling of liquid droplets suspended in an aerodynamic levitator. Application of the levitator has been reported in our previous work on aluminate liquids [13, 14]. Samples were made from high-purity mixtures of calcium carbonate and aluminium oxide powder, which were milled, fused and milled again to achieve homogenization of the mixture. Portions of this mixture were then fused into about 3 mm diameter spheroids using a CO_2 laser beam [15]. Approximately 40 glass spheroids were synthesized to provide about 2 g of glass material. About half of the eutectic glass was saved for use in the structure studies and half was partially crystallized by heat treatment at 1600 K for 16 h. The densities of the glasses were measured using a pycnometer with perfluoromethyldecalyn as the immersion fluid. The compositions of the glasses were confirmed by microprobe analysis.

Pulsed neutron diffraction measurements were made on the Glass, Liquid and Amorphous Diffractometer (GLAD) at the Intense Pulsed Neutron Source (IPNS), Argonne National

Laboratory [16]. About 1 g of coarsely crushed glass or partially crystalline material was contained in a thin-walled (0.1 mm) vanadium tube with an inner radius of 3 mm. Neutron measurements were also performed on the instrumental background, a 6 mm diameter solid vanadium rod and the empty sample container.

High-energy x-ray measurements were performed using 1×1 mm^2 $\sim$115 KeV beams on the BESSRC-CAT, ID-11-C beamline at the Advanced Photon Source (APS) [17]. The same samples were contained in a 4 mm wide aluminium frame with 10 μm Mylar windows arranged such that only the sample and the windows were in the path of the x-ray beam. Background measurements were made on the same part of the Mylar window with the sample removed to obtain the scattering contribution from the container. The use of high-energy x-ray instrumentation enables experiments with very low x-ray attenuation and multiple-scattering factors (a few per cent) and accesses a high momentum transfer range.

4. Data analysis

In the neutron scattering data analysis, corrections were made for container scattering, attenuation, multiple scattering and inelastic scattering and the data were normalized to the scattering from a vanadium rod. This was performed using the ATLAS software package for time-of-flight neutron diffraction data [18]. For the x-ray data analysis, corrections were made for detector dead-time, container scattering and Compton scattering. The software program ISOMER-X [19] was used to reduce the high-energy x-ray diffraction data. At the high x-ray energies used, the x-rays act as a bulk probe and attenuation and multiple-scattering effects were assumed to be negligible. Relativistic corrections were applied at high Q using the Klein–Nishina formula [20]. The incident x-ray beam energy was calibrated independently from our diffraction measurements using a radioactive source. This worked well for the 50:50 sample data, but for the 64:36 sample measurement there was a slight drift in beam energy and it was necessary to reduce the measured incident beam wavelength by 1.5% to obtain exact agreement with the neutron Al–O bond distance for the same sample. The neutron scattering lengths were obtained from Sears [21] and the atomic form factors and Compton scattering from the tabulated values of Hubbell [22]. The measured number density, for both glasses, was found to be 0.074 atoms Å^{-3} and a density of 0.069 atoms Å^{-3} was used for the polycrystalline sample based on the low-r limit of the neutron $G(r)$. No evidence of Bragg scattering was observed in either the high-angle (high-resolution) neutron detector banks or in the x-ray scattering experiments.

5. Experimental results

The measured neutron and x-ray structure factors are presented in figures 1 and 2, respectively. The previous neutron data of Hannon and Parker for a 38 mol% Al_2O_3 composition glass [4] and x-ray data of Morikawa *et al* on a 36.8 mol% Al_2O_3 glass [9] are also shown. The agreements with our measured Q-space data and the literature curves are qualitatively similar. However, there are significant differences in the coordination numbers reported from the real-space Fourier transforms.

The $S_N(Q)$ for the partially polycrystalline (eutectic composition) sample is presented in figure 3. Using the neutron data and the results of conventional x-ray diffraction measurements on the partially crystallized glass sample, two crystalline phases were identified: $Ca_{12}Al_{14}O_{33}$ (mayenite) and $CaAl_2O_4$ (calcium monoaluminate) [8, 10]. No evidence was found of calcium trialuminate [23]. In figure 4, the corresponding real-space functions for the glass

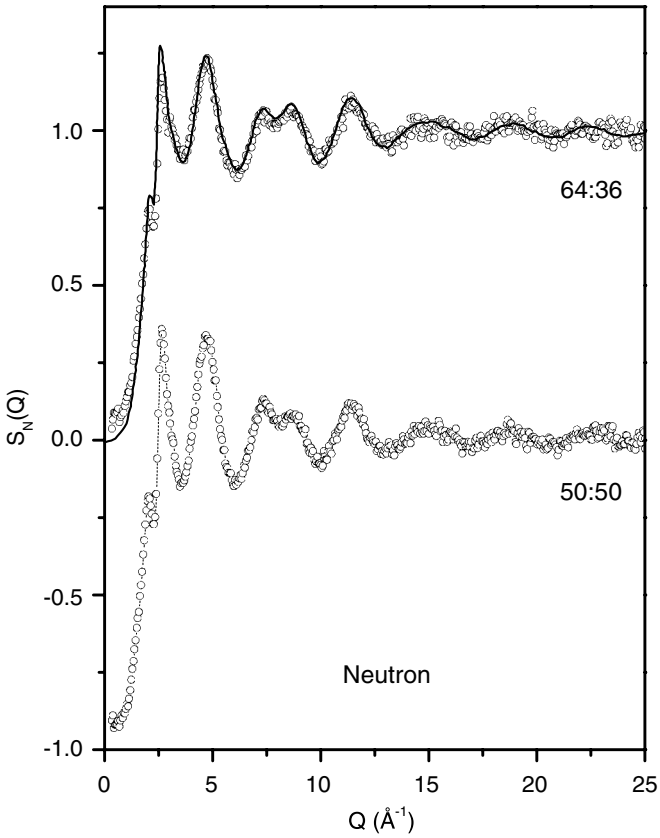

Figure 1. The measured neutron structure factor $S_N(Q)$ (circles) for the quenched CA eutectic and equimolar (shifted by −1) glasses. Previous neutron data on a splat-quenched 38 mol% Al_2O_3 glass of Hannon and Parker [4] are shown as a solid curve overlaying the 64:36 composition (top curve).

and polycrystalline eutectic compositions, $G_N(r)$, are compared. The nearest-neighbour Al–O coordination number was obtained by fitting the neutron curves with single-Gaussian distributions in $G_N(r)$. At the eutectic composition, aluminium was found to be coordinated by 4.8(1) oxygens in the glass and 4.3(1) in the crystal. This coincides with a slight shift in peak position from 1.76(1) Å in the glass to 1.75(1) Å in the polycrystalline sample. In contrast, a single-Gaussian fit to the first peak in $G_N(r)$ for the equimolar composition glass gave an Al coordination number of $n_{Al}^{O} = 4.0(1)$ centred on an average bond length of 1.76(1) Å (see figure 5).

The second peak in $G_N(r)$ corresponds to the Ca–O bond, which was found to be at a distance of 2.34(2) Å in the glass and 2.40(2) Å in the polycrystalline sample. In the neutron data this peak is significantly diminished in intensity at the equimolar composition and cannot easily be resolved (figure 5). Moreover, the second (CaO) peak position for the eutectic composition is at 2.34(2) Å in the neutron data and 2.36(2) Å in the x-ray data. In the x-ray spectra however, the CaO peaks for the two compositions appear comparable in intensity (see figure 6), suggesting there are significant overlaps of O–O contributions in this region of the neutron data.

At higher r in the neutron correlation function there is a strong O–O peak at 2.89 Å followed by two smaller peaks around 4.2 and 4.5 Å. In the x-ray spectra, the O–O peak is not clearly

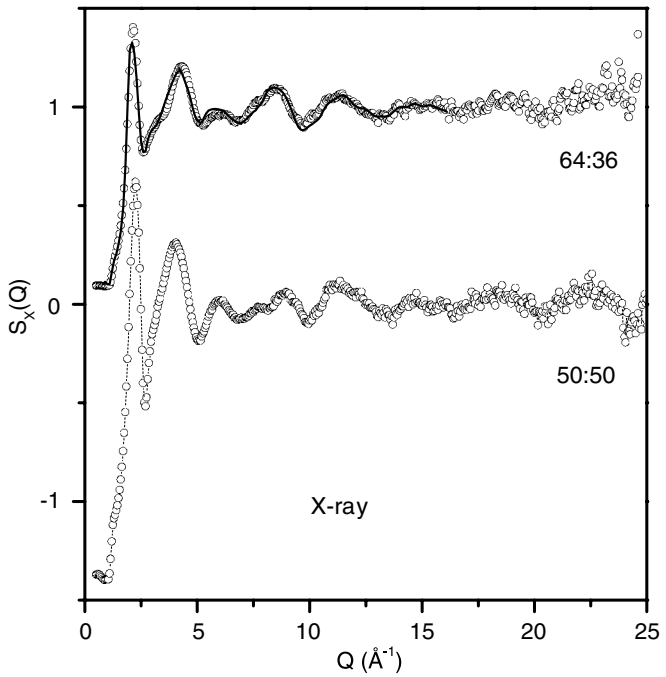

Figure 2. The measured x-ray structure factor, $S_X(Q)$ (circles), for the laser-quenched CA eutectic and equimolar (shifted by -1) glasses. Previous x-ray data on a splat-quenched 36.8 mol% Al_2O_3 glass (see [9]) are shown as a solid curve overlaying the 64:36 composition (top curve).

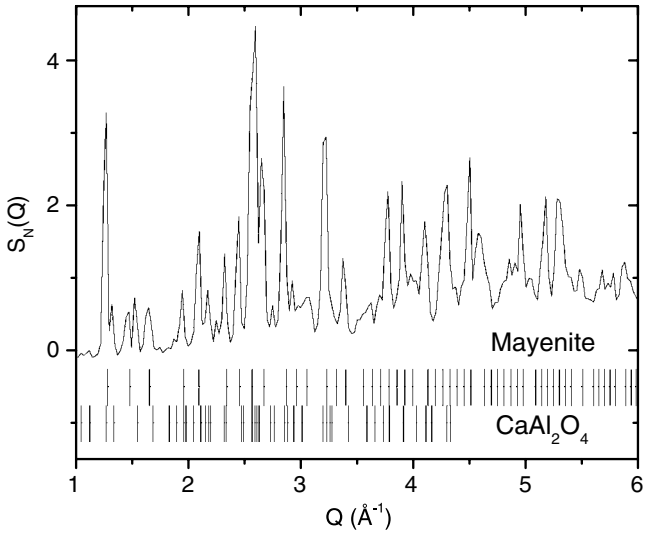

Figure 3. The neutron structure factor for the partially polycrystalline CA eutectic composition material is shown together with the Bragg peak positions of crystalline mayenite and calcium monoaluminate.

observed, but rather the heavier Al and Ca nearest-neighbour atom correlations dominate. The region of 3–4 Å in the x-ray data shows the main differences in connectivity between the two samples, albeit rather subtle, and this region is discussed in more detail in the next section after

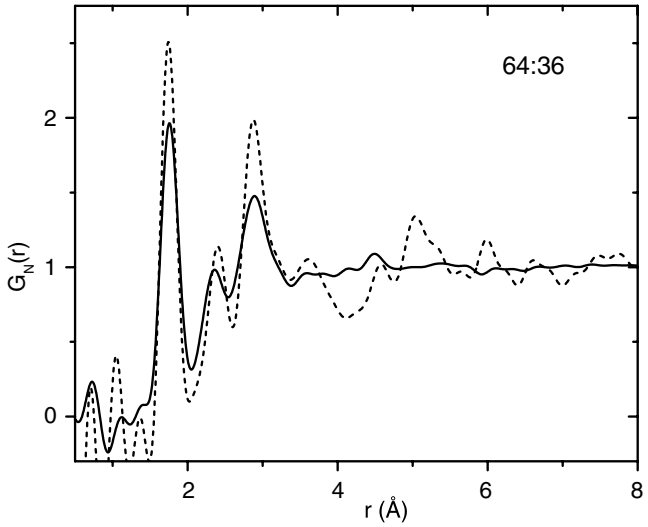

Figure 4. The radial distribution functions $G_N(r)$ for the CA eutectic (obtained by Fourier transformation of the corresponding curves in figures 1 and 3) are shown as a solid curve (glass) and a dashed curve (partially crystalline).

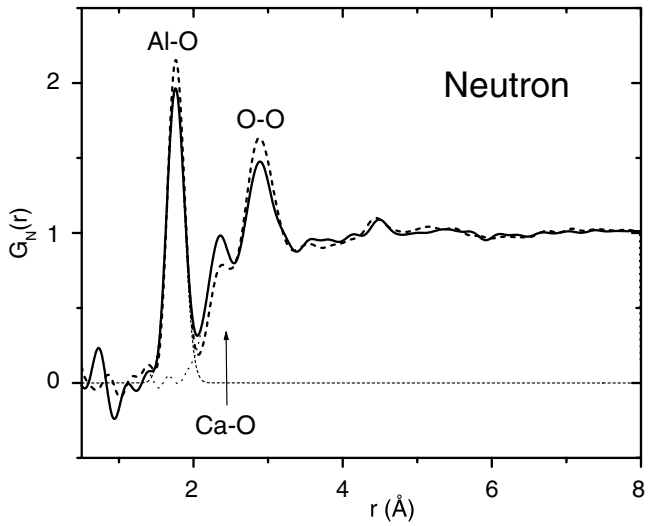

Figure 5. The real-space neutron $G_N(r)$ radial distribution functions for the CA eutectic (solid curve) and equimolar glasses (thick dashed curve). A typical Gaussian fit to the data (thin dashed curve) used to determine the coordination number together with the residue function are also shown (dotted curve).

further analysis. The two smaller peaks observed around 4.2 and 4.5 Å in the neutron spectra are also seen in the x-ray spectra, suggesting that they may be oxygen-related correlations.

6. Discussion

Analysis of the polycrystalline material shows a number of structural similarities between the glass and crystalline phases. For the compositions investigated, the crystalline phases

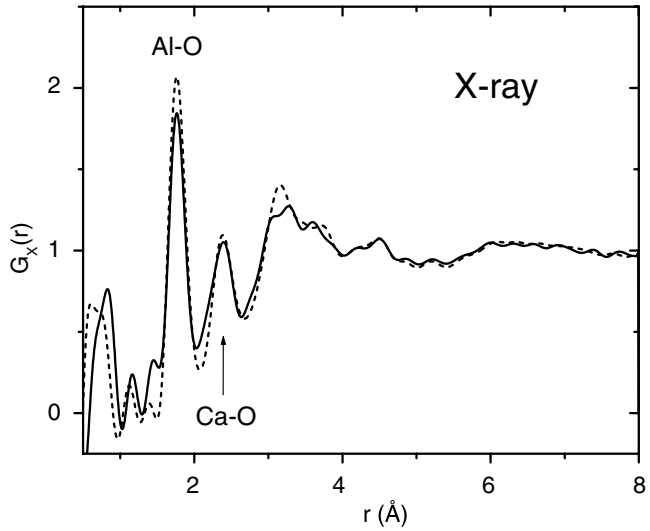

Figure 6. The real-space x-ray $G_X(r)$ radial distribution functions for the CA eutectic (solid curve) and equimolar glasses (dashed curve).

identified were mayenite ($Ca_{12}Al_{14}O_{33}$) [11] and calcium monoaluminate ($CaAl_2O_4$) [24]. The latter comprises sixfold rings of distorted AlO_4 tetrahedra, with the Ca atoms taking up positions in the holes between the rings, with three Ca atom positions. Two of these are sixfold coordinated by oxygen at a mean distance of 2.36 Å and the third is ninefold coordinated by oxygen at distances ranging from 2.36 to 3.17 Å, with the nearest six oxygens forming an elongated octahedron. Mayenite comprises a network of corner-sharing chains of interlinked AlO_4 tetrahedra and both sixfold and sevenfold Ca polyhedra [10], with CaO bonds of 2.36–2.52 Å.

The $G_N(r)$ functions for the eutectic glass shown in figure 4 indicate a strong correlation at ∼1.77 Å associated with Al–O species. The sum of the ionic radii of four-coordinate Al and O is 1.77 Å based on values given by Shannon and Prewitt [25]. However, the Al–O coordination numbers of 4.0 (equimolar) and 4.8 (eutectic) found in this study suggest that a range of differently coordinated Al units can exist in the glassy $CaO:Al_2O_3$ system. The latter value of $n_{Al}^{O} = 4.8$ at the eutectic composition differs significantly from the value of 4.0 obtained by Hannon and Parker [4] (obtained for splat-quenched glasses whose compositions bracket the eutectic composition). It is also higher than the value of 4.2 found by Morikawa *et al* [9] for a 36.8 mol% Al_2O_3 splat-quenched glass. More importantly, it is opposite to the expected trend of increasing Al coordination with increasing Al content, as found in the ion dynamics simulations of Poe *et al* [10], which were in qualitative agreement with their ^{27}Al NMR results. The most reasonable explanation for the difference is the change in preparation conditions of the glassy samples.

The neutron/x-ray Q-space difference functions shown in figure 7 were constructed to eliminate the O–O correlations to observe any higher-order Ca–O correlations, using the formula given in equation (6). The corresponding real-space curves are given in figure 8. For the eutectic composition calcium is found to be coordinated on average by 3.9(2) oxygens at 2.40 Å, whilst at the equimolar composition this increases to 5.6(2) at 2.38 Å. The eutectic data are in good agreement with the value of $n_{Ca}^{O} = 4.0$ found by Hannon and Parker [4], but considerably lower than the value of 5.6 observed by Morikawa *et al* [9]. It is interesting to note that there are no additional higher CaO correlations found to exist between 2.4 and 2.7 Å

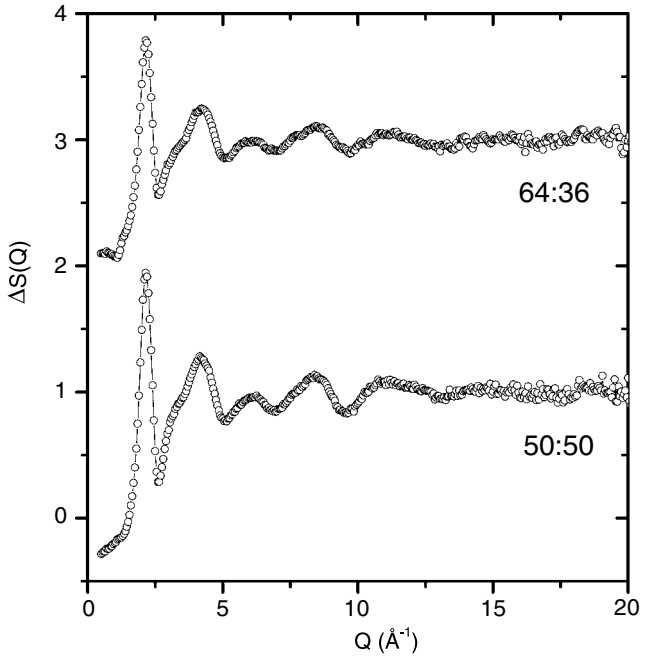

Figure 7. Reciprocal-space x-ray/neutron difference functions for the eutectic and equimolar glass compositions. $\Delta S(Q)$ is similar to the measured x-ray data but corresponds to a function in which the O–O interactions have been completely eliminated (see equation (3)).

(see figure 7). This does not preclude the existence of longer Ca–O correlations >2.7 Å at the eutectic composition, which may be masked by other correlations.

In the region of 3–4 Å at the eutectic composition the difference function has a shoulder at ∼3.1 Å followed by two well defined peaks at 3.29 and 3.60 Å and another shoulder at ∼3.9 Å, whilst in the equimolar glass data there are two well defined peaks at 3.18 and 3.72 Å, possibly with a small feature between them at 3.45 Å. Since the Al–Al intensity is expected to be higher in the equimolar glass, the 3.18 Å peak may be assigned to Al–Al interactions from corner-sharing tetrahedra. This peak shifts to 3.29 Å in the eutectic glass (where fivefold Al polyhedra dominate) and the low-*r* shoulder at ∼3.1 Å may arise from corner-sharing tetrahedra Al–Al interactions and/or additional Ca–O correlations. On the basis of ion size, the higher-*r* correlations between 3.45 and 3.9 Å are probably due to Ca–Al and Ca–Al interactions.

The implications of the low and/or distorted Ca coordination are that the Ca ion may contribute to the network development, accounting for the relatively easy glass formation observed in this system. The observation that the ion–ion distributions beyond 3.7 Å remain almost identical in the two glasses, despite the differences in local structure, lends support to this idea, i.e. that both the Ca and Al ions may act as network formers in these glasses.

7. Conclusions

Containerless methods have been used to produce quenched 64:36 mol% eutectic and 50:50 mol% CaO:Al_2O_3 eutectic glasses. Detailed structural pictures of the glass have been obtained using a combination of pulsed neutron diffraction and high-energy x-ray diffraction methods. The results indicate that the equimolar glass is, on average, composed mainly of

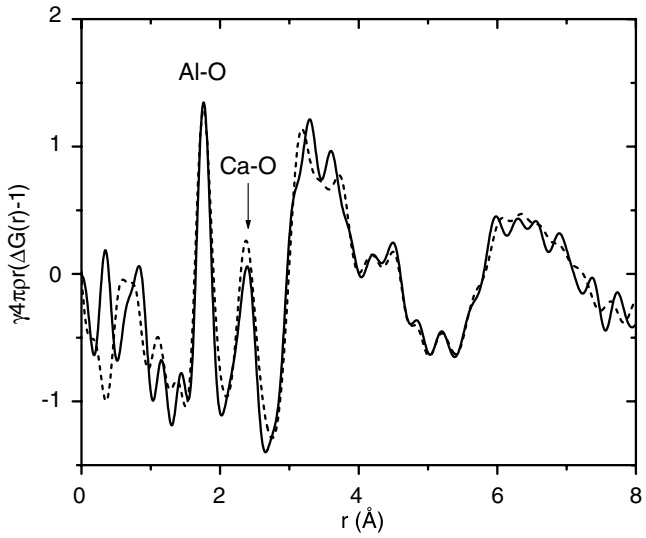

Figure 8. Real-space x-ray/neutron difference functions for the eutectic (solid curve) and equimolar (dashed curve) glass compositions shown in figure 6. $\Delta G(r)$ corresponds to a function in which the O–O interactions have been eliminated, to obtain information on the CaO distances. For the eutectic $\alpha = 1$ and for the equimolar composition $\gamma = 0.72$, reflecting the ratio of Al_2O_3 content in the glasses.

AlO_4 tetrahedra and the eutectic composition glass is dominated by a mixture of both AlO_4 and AlO_5 polyhedra. In a dramatic change, the average calcium coordination decreases from 5.6(2) oxygens in the $CaAl_2O_4$ glass to 3.9(2) oxygens at the eutectic composition, despite only a 0.02(1) Å shift in the Ca–O bond length. Although higher Ca–O correlations beyond 2.7 Å may also exist, the Ca coordination is either unusually low or highly distorted in the 36 mol% composition. Whilst it is unexpected that the coordination of Al increases with decreasing Al content in these glasses, this increase may be understood in terms of the Ca ion 'donating' oxygen to the aluminium. If this is true, it follows that both the Ca and Al ions may act as network formers in these glasses.

Acknowledgments

Neutron scattering experiments were carried out at the Intense Pulsed Neutron Source and the high energy x-ray experiments at the Advanced Photon Source; both facilities are based at Argonne National Laboratory. IPNS and BESSRC-CAT are operated under the auspices of the US Department of Energy, Basic energy sciences, and funded under contract number W-31-109-ENG-38. Work at CRI was supported by NASA Physical Sciences Division under contract number NAS8-00125. We thank Joerg Neuefeind, Mark Beno and Yang Ren for help with the x-ray experiments and Ms Kirsten Hiera and Mr Thomas Key for help with materials synthesis and density measurements.

References

[1] Shepherd E S, Rankin G A and Wright F E 1909 *Am. J. Sci.* **28** 293
[2] Nurse R W, Welch J H and Majumdar A J 1965 *Trans. Br. Ceram. Soc.* **64** 416
[3] Poe B T, McMillan P F, Cote B, Massiot D and Coutures J-P 1994 *J. Am. Ceram. Soc.* **77** 1823

[4] Hannon A C and Parker J M 2000 *J. Non-Cryst. Solids* **274** 102
[5] Uhlmann E V, Weinberg M C, Kreidl N J, Burgner L L, Zanoni R and Church K H 1994 *J. Non-Cryst. Solids* **178** 15
[6] de Souza D F, Sampaio J A, Nunes L A O, Baesso M L, Bento A C and Miranda L C M 2000 *Phys. Rev.* B **62** 3176
[7] Paradis P-F, Babin F, Gagne J-M and Levesque S 1997 *J. Opt. Soc. Am.* B **14** 1009
[8] Ampian S G 1964 *US Bureau of Mines Report* 6428
[9] Morikawa H, Marumo F, Koyama T, Yamane M and Oyobe A 1983 *J. Non-Cryst. Solids* **56** 355
[10] Poe B T, McMillan P F, Cote B, Massiot D and Coutures J-P 1993 *Science* **259** 786–8
[11] Christensen A N 1987 *Acta Chem. Scand.* A **41** 110–12
[12] Keen D A 2001 *J. Appl. Crystallogr.* **34** 172–7
[13] Weber J K R and Nordine P C 1995 *Micrograv. Sci. Technol.* **7** 279–82
[14] Weber J K R, Hixson A D, Abadie J G, Nordine P C and Jerman G A 2000 *J. Am. Ceram. Soc.* **83** 1868–72
[15] Weber J K R, Felten J J and Nordine P C 1996 *Rev. Sci. Instrum.* **67** 522
[16] Ellison A J G, Crawford R K, Montague D G, Volin K J and Price D L 1993 *J. Neutron Res.* **4** 61
[17] Rütt U, Beno M A, Stempfer J, Jennings G, Kurtz G and Montano P A 2001 *Nucl. Instrum. Methods* A **467** 1026–9
[18] Soper A K, Howells W S and Hannon A C 1989 *Rutherford Appleton Laboratory Report* RAL 89-046
[19] Urquidi J, Benmore C J, Neuefeind J and Tomberli B 2003 *J. Appl. Crystallogr.* **36** 368
[20] Klein O and Nishina Y 1929 *Z. Phys.* **57** 853
[21] Sears V F 1992 *Neutron News* **3** 26–37
[22] Hubbell J H, Veigele W J, Briggs E A and Howerton R J 1973 *J. Phys. Chem. Ref. Data* **4** 471
[23] Mondal P and Jeffery J W 1975 *Acta Crystallogr.* B **31** 689–97
[24] Doughill M W 1957 *Nature* **180** 292–3
[25] Shannon R D and Prewitt C T 1969 *Acta Crystallogr.* B **25** 925